Article

Spatiotemporal Distributions and Vulnerability Assessment of Highway Blockage under Low-Visibility Weather in Eastern China Based on the FAHP and CRITIC Methods

Tian Jing [1,2], Duanyang Liu [2,*], Yunxuan Bao [1,2,3,*], Hongbin Wang [2], Mingyue Yan [2,4] and Fan Zu [2]

1   Collaborative Innovation Center on Forecast and Evaluation of Meteorological Disasters, Nanjing University of Information Science & Technology, Nanjing 210041, China; jingtian819216471@163.com
2   Key Laboratory of Transportation Meteorology of China Meteorological Administration, Nanjing Joint Institute for Atmospheric Sciences, Nanjing 210017, China
3   Engineering Research Center for Internet of Things Equipment Super-Fusion Application and Security in Jiangsu Province, Wuxi University, Wuxi 214105, China
4   Highway Monitoring & Response Center, Ministry of Transport of the People Republic China, Beijing 100029, China
*   Correspondence: liuduanyang@cma.cn (D.L.); baoyunxuan@163.com (Y.B.)

Abstract: In this study, the spatiotemporal distributions of highway blockage and the low-visibility weather events in eastern China are studied by taking Jiangsu Province as an example. Based on the record table data of highway-blocking events, a vulnerability evaluation model for the highway network in Jiangsu Province is established using the weight assignment methods of the fuzzy analytic hierarchy process (FAHP) and criteria importance though intercriteria correlation (CRITIC). By using the geographic information system, the vulnerability evaluation map of road network in low-visibility weather in Jiangsu Province is finally drawn. The results show that the monthly blockage events on Jiangsu highways are more frequent in the north than in the south and are more frequent along the coast than inland, with the highest occurrence number in winter and a second peak in May. There are basically no blockage events from July to October. Traffic blockage on Jiangsu highways mainly occurs between 22:00 and 08:00 Beijing time. In the afternoon, there are almost no highway-blocking events caused by low-visibility weather. The vulnerability of highway blockage in Jiangsu Province is high in the north and low in the south and high in coastal areas and relatively low in inland. The section K6-K99 of the G30 Lianhuo Highway is the most sensitive.

Keywords: highways; road blockage; fuzzy analytic hierarchy process; CRITIC weight assignment method; road network vulnerability; spatiotemporal distribution

1. Introduction

Traffic blockage is a prolonged obstruction or blockage of road access due to sudden traffic-related events, which may be caused by issues such as severe weather, geological disasters, traffic accidents, and planned traffic blockage (road and bridge maintenance, major social events, etc.) [1–3]. Concurrent with the rapid development of China's economy, the mileage and traffic flow of highways have also experienced rapid growth. Prolonged traffic blockage affects the flow, increases the risk of major accidents, threatens the lives of drivers, and has negative impacts on social and economic development [4]. Research has shown that rainfall, snow, fog, and typhoons can all lead to highway blockages [5]. Researchers have found that among all the adverse weather conditions, low visibility causes the greatest hazards during vehicle operation [6]. Many studies have demonstrated that approximately a quarter of all traffic blockages are caused by low-visibility weather, such as dense fog, and the rate of highway accidents in dense fog is 10 times higher than that in normal weather [7].

Low-visibility weather is a catastrophic weather phenomenon in which horizontal visibility is reduced to less than 1000 m by heavy precipitation (e.g., water droplets or ice crystals), fog, etc. [8]. On 15 November 2017, the Chu-Xin highway in Anhui Province was affected by dense fog. More than 30 vehicles collided in succession, and the road was severely blocked. On the morning of 28 January 2021, a series of car crashes occurred on section 1026 of the Hu-Chong highway in Qianjiang, Hubei Province, which was also caused by dense fog. Approximately 20 vehicles were involved in a pileup, which caused a prolonged highway-blocking event [9].

There are many studies regarding the incidence, severity, and risk of highway crashes caused by low-visibility weather [10,11]. Hamilton et al. [12] and Abdel-Aty et al. [13] found that drivers are more likely to be involved in fatal crashes while driving in low-visibility weather. Alghamd et al. [14] used Poisson regression to analyze the 30-year crash data and found that the severity of crashes on foggy days is over 2.55 times higher than on other days. Perry et al. [15] found more severe crashes related to low visibility on highways than that on other roads. Wu et al. [16] applied a binary logistic regression model to actual traffic flow and weather data from two areas in Florida to compare the traffic patterns during persistent fog events to those during sunny periods. Their results show that the risk of accident increases under foggy conditions. Feng et al. found there is a high correlation between the variations of fog-related traffic accidents and low-visibility weather on four highway sections in China [17]. By analyzing the traffic accidents and associated weather conditions in England and Wales, Edwards et al. found that there is an obvious seasonal variation of traffic accidents [18].

Many researchers conducted studies on the traffic vulnerability of roads. Berdica [19] proposed a definition of vulnerability for the road traffic network for the first time, which refers to the vulnerability factors of the road network to adverse external influences. Husdal et al. [20] considered the road network vulnerability as the non-functionality of the road transport network under certain circumstances, emphasizing the loss or impact of an event on the network. Sohn [21] and Scott [22] proposed a scenario-based approach which can identify the key locations in the road network and investigate the vulnerability of the network. Huang et al. [23] explored the factors influencing the degree of injury and death in traffic accidents through the aspect of accident severity. Christopher et al. [24] studied the impact of environment on the safe driving of electric bicycles based on the traffic statistics from the National Statistical Yearbook. Wang et al. [25] used questionnaires to obtain the information on the driving safety of e-bike drivers. Yu et al. [26] analyzed the impact of traffic speed on traffic safety by acquiring vehicle speed information based on coil detectors. There are also many methods of machine learning [27] and computational intelligence [28,29] that have been applied to the analysis and identification of traffic accident risk.

The whole vulnerability assessment mainly refers to the definition of vulnerability to the catastrophe, including three parts: indicator screening, indicator empowerment, and evaluation methods [30]. Among them, the combination of subjective and objective methods was adopted in the index weighting. The subjective method is the fuzzy analytic hierarchy process (FAHP), which optimizes the weight calculation process and can achieve the consistency of judgment matrix and the unity of the thoughts of decision makers [31]. The method of criteria importance though intercriteria correlation (CRITIC) is adopted for objective weighting, which has more adaptability in the weighting for indicators with stronger relevance [32]. The combination of subjective and objective weighting methods can make up for the shortcomings of a single method and solve the defects of a single evaluation method. This combination model has been widely used in the assessments of natural disaster risk, natural resources and carrying capacity [33].

Much of the research on the impact of low-visibility weather on highways is focused on the traffic accident rate or traffic flow, while the research on traffic blockage is mainly focused on the macroscopic level, lacking detailed analysis on the specific types of catastrophic weather. There is no good method for evaluating the vulnerability of motorway

networks and no specific study on the vulnerability of road network under specific weather hazard. There is also no specific spatial matching method for the low-visibility weather and motorway-blocking events.

To address the abovementioned problems, this study uses highway control needs as guidance and takes the highway-blocking events under low-visibility weather conditions in Jiangsu Province as the main research object. Instead of lumping all weather factors into one category, we select low-visibility weather—which accounts for a relatively high proportion of highway weather hazards in eastern China—as the target weather type, filter out all the low-visibility weather events that cause highway blockage, and propose a corresponding model to evaluate the vulnerability of the road network to specific weather hazards. Different weather events require specific response measures, which can effectively improve the efficiency of disaster prevention and mitigation and reduce the cost of emergency management. The aim of this work is to improve the existing theory of highway traffic blockage and provide technical support to ensure the smooth and safe operation of regional highway traffic.

The rest of this paper is organized as follows. The materials and methods are described in Section 2. The highway blockage characteristics, distribution of low-visibility weather, and blockage vulnerability are analyzed in Section 3. Finally, the discussions and main conclusions are given in Sections 4 and 5, respectively.

2. Materials and Methods

2.1. Study Area

The study area is Jiangsu Province (166°18′–121°57′ E and 30°45′–35°20′ N), which is located in the eastern part of the Jianghuai Plain along the coast of mainland China and in the mid-latitude zone along the east coast of the Asian continent. This region is in the climate transition zone between the subtropical and warm temperate zones and is characterized by the East Asian monsoon climate. However, it is influenced both by the westerlies in the middle latitudes and the easterlies in subtropical and low latitudes, thus causing a variety of meteorological disasters. There is a network of more than 50 highways (approximately 5000 km in total) in Jiangsu Province, as shown in Figure 1, which suffers from low-visibility weather more and more frequently in recent years. Traffic blockage due to fog and other low-visibility conditions has occurred repeatedly. Therefore, the road safety problems caused by low visibility have received close attention from all sectors of society [34].
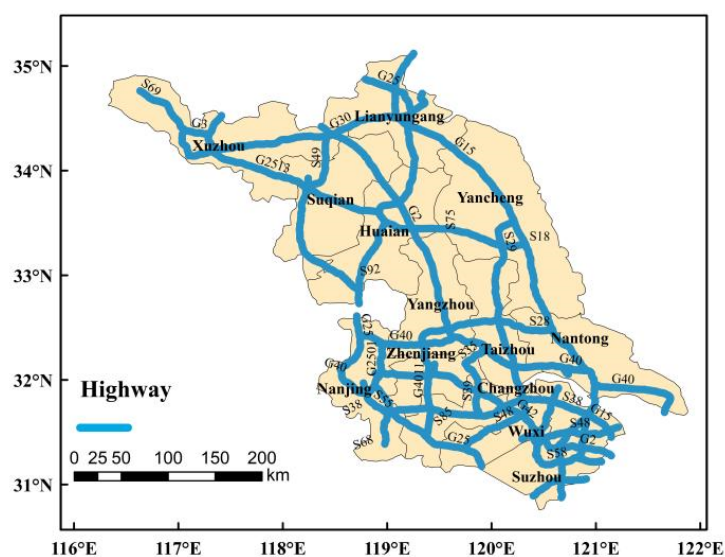

Figure 1. Distribution of highway networks in Jiangsu Province.

2.2. Traffic Blockage Data

The traffic blockage data used in this study are the records of traffic disruptions on the highway network in Jiangsu Province in 2020 obtained from the Road Network Monitoring and Emergency Response Centre of the Ministry of Transport. The records follow the standards established by the Ministry of Transport Highway Traffic Blockage Information Reporting System (Transportation Highway Development (2006) No. 451). There are 16 items in the records, including the province, reporting unit, route name, route number, starting and ending 100 m distance marker, reason for the blockage, length (mileage) of the blockage, status, blockage type, information event classification, site description, disposal measures, blockage discovery time, reporting time, and expected recovery time. Considering that highway blockage information is reported manually, there may be statistical errors in the records. The time series of data are corrected in advance, and then data quality control is performed based on the revised correlation of blockage causes and site descriptions.

2.3. Research Methodology

2.3.1. Determination of Blockage Events Caused by Low-Visibility Weather

In addition to low-visibility weather, the causes of highway blockages include rainfall (water), snowfall (snow), icy roads, and other factors. However, this study focuses on highway blockages caused by low-visibility factors. In order to pinpoint the location of the section where the blockage event occurs, geographic information systems (GIS) technology is used to analyze each blockage event, and the maximum segmentation unit selected in this study is 1 km.

The specific analysis steps are shown in Figure 2. In Part 1, the SPLIT function module in Python is used to slice the data in the record table, and the matching function is used to calibrate and match the road network data with the highway blockage events data. In Part 2, GIS technology is used to spatially match the blockage events with the highway network and visualize the spatial distribution.
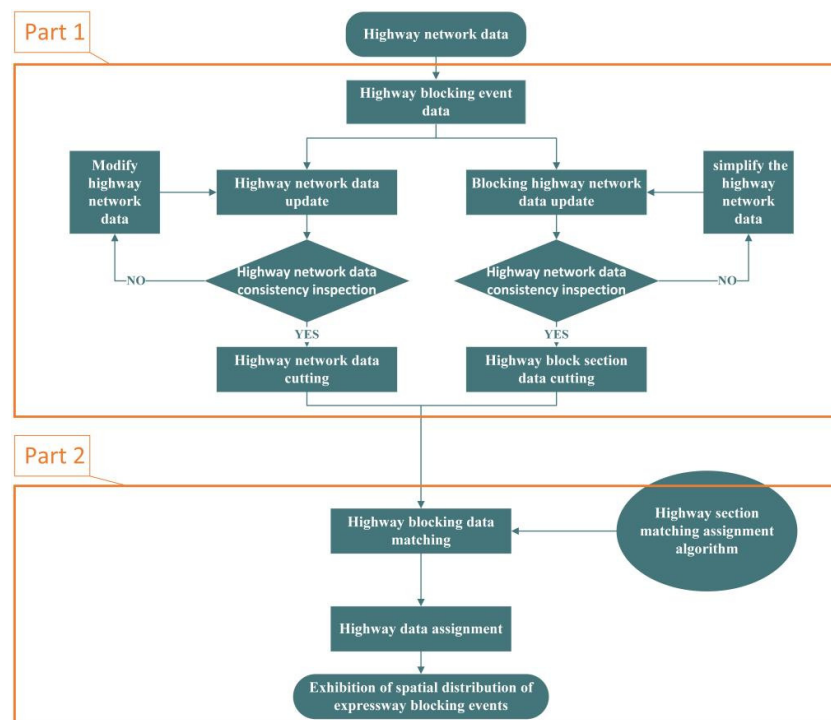

Figure 2. Flow chart of matching assignment of highway block sections.

Data pre-processing is performed first. New highway data are generated through the integration of national and provincial highway route codes. To correct the manually recorded highway blockage data, each highway blockage event in the spatial data of the highway network is analyzed by using the correlation between the route codes and pile numbers, and the incorrect blockage events are removed. The POINT_REMOVE simplification algorithm of GIS platform is then used to simplify the highway network data.

The SPLIT function is used as a processing tool for each blockage event on each highway section with a cell length of 1 km. First, each highway blockage is matched with the corresponding highway data since the starting and ending points of each blockage event are known. Then, the corresponding event is plotted spatially via GIS and attributed with the appropriate information from the nearest highway marker. Traffic events are counted as multiple events if the starting and ending markers that demarcate the extent of the event include more than one section. Each section between the markers is therefore counted as one event.

Based on the occurrence frequency of traffic blockage events under low-visibility weather in 2020, this study classifies the highway sections into six levels: slight risk (<8), less risk (8–14), medium risk (15–21), severe risk (22–28), more severe risk (29–35), and extreme risk (>35).

2.3.2. FAHP Weight Assignment Method

In order to evaluate the vulnerability of the highway network in Jiangsu Province under low-visibility weather, the FAHP method is used to obtain the subjective weights for the analysis of vulnerability weight. The results can be used as one of the reference indexes for the final analysis of vulnerability [35,36].

Based on the hierarchical analysis (AHP), the problem and influencing factors are characterized into the three layers of target, criterion, and indicator. Secondly, the indicator factors u_1–u_n with the same affiliation and hierarchy are compared in pairs to measure their importance, and the scale of importance is represented by 1 to 9 and its reciprocal. The judgment matrix $H_{n \times n}$ is established though Equation (1):

$$H_{n \times n} = \left(a_{ij} \right)_{n \times n} \tag{1}$$

In Equation (1), a_{ij} is the AHP importance scale of u_i and u_j relative to the upper factors, in which a_{ii} is equal to 1 and a_{ji} is the reciprocal of a_{ij}. The meanings of the importance scales are shown in Table 1.

Table 1. Meanings of importance scales.

Scale	Description
1	Equally important
3	Slightly important
5	Obviously important
7	Strongly important
9	Extremely important
2, 4, 6,8	Median value

According to the scale conversion formula, the judgment matrix is transformed into a fuzzy complementary judgment matrix $W_{n \times n}$ though Equations (2) and (3):

$$w_{ij} = log_\alpha a_{ij} + 0.5 \tag{2}$$

$$W_{n \times n} = \left(w_{ij}\right)_{n \times n} \tag{3}$$

where a_{ij} is the same variable as that in Equation (1). α can be used to adjust the difference between the weights of the final indicators, which is determined by the decision maker according to the actual situation. In this study, α is set to be equal to or greater than 81 to ensure that the w_{ij} is between 0 and 1. It can be seen from Equation (2) that w_{ij} represents the relative importance of u_i and u_j and that $w_{ij} + w_{ji}$ is equal to 1. When w_{ij} is equal to 0.5, u_i and u_j are of equal importance; when w_{ij} is greater (less) than 0.5, u_i (u_j) is more important than u_j (u_i).

The fuzzy complementary judgment citation is further transformed into the fuzzy consistent judgment matrix $R_{n \times n}$ through the following equations:

$$r_i = \sum_{j=1}^{n} w_{ij} \tag{4}$$

$$r_{ij} = \frac{r_i - r_j}{2(n-1)} + 0.5 \tag{5}$$

$$R_{n \times n} = \left(r_{ij}\right)_{n \times n} \tag{6}$$

where r_{ij} is the FAHP importance scale of u_i and u_j corresponding to the upper factors, and it satisfies the conditions of $r_{ii} = 0.5$, $r_{ij} + r_{ji} = 1$ and $r_{ij} = r_{ik} - r_{jk} + 0.5$, $(i, j, k = 1, 2, \ldots, n)$.

The fuzzy judgement matrix is consistent with no need for consistency testing, and it can reflect the subjective thought of the decision maker. The subjective weight W_1 corresponding to each indicator can be obtained via the characteristic root method.

2.3.3. CRITIC Weight Assignment Method

Considering that there is a strong correlation between the selected indicators, the CRITIC method was adopted in this study to objectively evaluate the vulnerability weight, which was regarded as one of the final vulnerability reference indicators [37].

The CRITIC method is an objective weight assignment method which is commonly used for the analysis of data with strong correlations between indicators while considering the variability among indicators concurrently. By objectively calculating the indicators of data, each indicator was assigned a different weight, and the calculation steps are as follows [38].

The standard deviation can be used to measure the contrast intensity and dispersion degree of indicators. A larger standard deviation represents a greater dispersion degree, which indicates larger differences between samples and larger assigned corresponding weights. The standard deviation can be calculated by Equation (7).

$$S_j = \sqrt{\frac{\sum_{i=1}^{n} \left(x_{ij} - \frac{1}{n} \sum_{i=1}^{n} x_{ij}\right)^2}{n-1}} \tag{7}$$

where x_{ij} denotes the ith sample for the jth indicator, S_j is the standard deviation of the jth indicator, and n is the total number of samples for the jth indicator.

Correlation is expressed as the correlation coefficient between indicators. The stronger the correlation between indicators is, the more conflicting the indicators are and the higher the repetition rate of information expression. Therefore, the corresponding weights of the indicators can be reduced to a certain extent. The correlation coefficient R can be calculated in Equation (8).

$$R_j = \sum_{i=1}^{p} (1 - r_{ij}) \tag{8}$$

where R_j indicates the correlation coefficient of the jth indicator with the other indicators, r_{ij} denotes the correlation coefficient between the ith and jth indicators, and p is the total number of indicators.

The weight of the jth indicator W_{2j} can be obtained from Equation (9).

$$W_{2j} = \frac{S_j \times R_j}{\sum_{j=1}^{p} S_j \times R_j} \tag{9}$$

2.3.4. Portfolio Empowerment Method

The CRITIC method considers the correlation between indicators more and pays attention to the information content of the data itself, but it is easily affected by the two-level value. The subjective weight assignment will ignore the information brought by the data itself. Therefore, the combination of subjective and objective weight assignment methods can be used for more reliable and accurate evaluation.

After the subjective and objective weighting methods are used to determine the weight of the assessment indicators, the proportion of subjective and objective weights in the overall weight should be clarified to better reflect the difference in the importance between multiple assessment indicators. W_1 and W_2 are the weights derived from the FAHP and CRITIC methods. The combined weight was obtained using the linear combination, as shown in Equation (10).

$$W = \alpha W_1 + \beta W_2 \tag{10}$$

where α and β denote the weight allocation coefficients.

In order to find the best combined weight, the optimal weight assignment coefficients which minimized the standard deviation of W were obtained though the following equations:

$$x_i = \alpha_i W_{1i} + \beta_i W_{2i} \tag{11}$$

$$\delta = \sqrt{\frac{\sum_{i=1}^{j} (x_i - \sum_{i=1}^{j} \frac{x_i}{j})}{j}} \tag{12}$$

where j is the maximum of sample numbers and both α and β are between 0 and 1 and their sum is equal to 1.

3. Results

3.1. Characteristics of Highway Blockage

3.1.1. Annual Variation of Highway Blockage

Based on the causes, site descriptions, and treatment measures, a total of 1340 highway blockages due to the low visibility were extracted from highway blockage records in Jiangsu Province in 2020, with a total annual cumulative blockage mileage of 69,466.3 km. In addition, the cumulative monthly blockage mileage and monthly blockage frequency were calculated to analyze the spatial and temporal distributions of highway blockages in Jiangsu Province.

As shown in Figure 3, the proportions of annual highway blockage events that led to blockage mileage less than 100 km, between 100–200 km, and 200–300 km are 85.5, 9.8, and 4.7%, respectively. The blockage events with maximum cumulative mileage and frequency on the highways of Jiangsu Province in 2020 basically occurred in January and February, while the minimum values were observed in August and September, when there was 0 km of cumulative blockage and 0 events were reported. The frequency of blockage was higher in January, February, May, November, and December, when the mileage of individual

blockage was also higher. The number of blockage events in May shows a second peak, which is different from the decreasing trend observed in March–April.
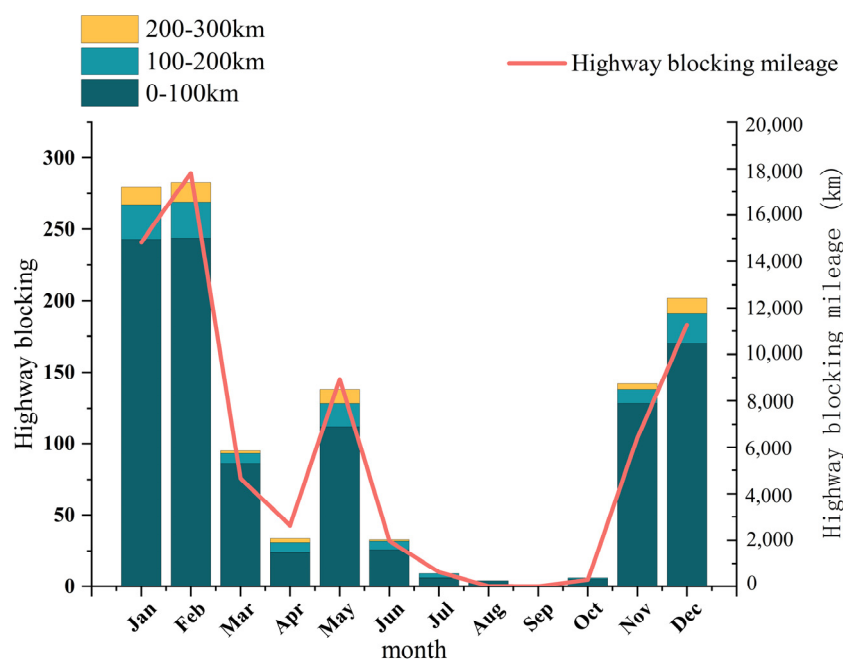

Figure 3. Annual variations of frequency (bars) and mileage (line) of highway-blockage events in Jiangsu Province in 2020.

The spatial distribution of highway blockage events in Jiangsu Province in 2020 (Figure 4) shows high occurrence in the north and low occurrence in the south. For the northern Jiangsu Province, the number of highway-blocking events in the eastern part is also substantially higher than that in the western part. It can be seen form Figure 4 that, as on the major north–south highways along the eastern coast and in the central region of Jiangsu Province, there are severe highway-blocking events in the north sections of the G15 Shenhai Highway and the G2 Beijing–Shanghai Highway. Among them, there are more than 37 blockage events in the K760–K1163 section of the G15 Highway, making this section one of the most severely blocked sections.

On the G25 Changshen Highway, the peak number of blockage events reached 64 in the K1762 section. The number of highway blockages in southern Suzhou was relatively small, with the cities of Wuxi (except Yixing) and Suzhou having four or fewer blockage events. There was no highway blockage on the S9 Sushao Highway and the G50 Shanghai–Chongqing Highway in Suzhou. There were at least 11 blockage events in Nanjing, Changzhou, and Yixing on the G25 Changshen Highway, sections K2060–K2190, in the western part of southern Jiangsu, which is a high value area within the entire southern Jiangsu region. Highway blockages in the central region of Suzhou were mainly concentrated in the K710–K1038 section of the G2 Highway. Niu et al. [39] conducted a GIS-based study on blocked highways in Jiangsu Province as a function of low visibility and found that the G15 Shenhai Highway is the key highway blocked by fog, which is basically consistent with the findings in this study.
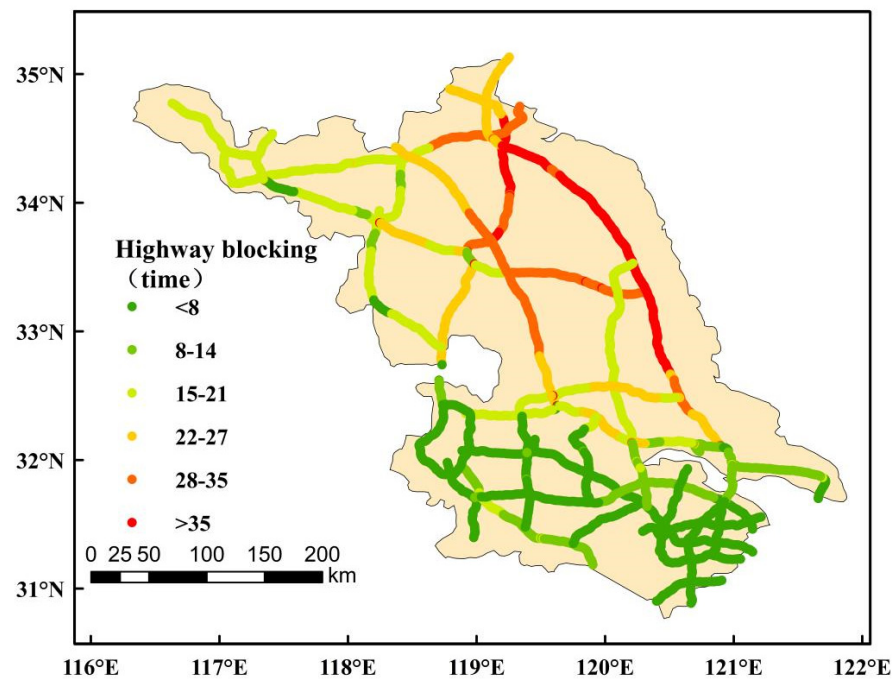
Figure 4. Spatial distribution of highway-blocking events in Jiangsu Province in 2020.

The annual variation of highway blockage spatial distribution in Jiangsu Province in 2020 (Figure 5) shows that there are more highway-blocking events in November, December, and January than that in other months, with 6–8 blockage events in January in the northern section of the G15 Shenhai Highway (K850–K989) and the central section of the G2 Beijing–Shanghai Highway (K712–K958). The southern section of the G15 Shenhai Highway K1090–K1173 was blocked less than the northern section, with six events. There were fewer than six blockage events in the southern part of Jiangsu Province, with most blockage occurring in the K43–K76 section of the S38 Changhe Highway in Wuxi (4–6 events). In February, the highway blockage is the most severe, with the highest number of 12 times on the G15 Shenhai Highway in Lianyungang and 10 blockage events occurring on the S18 Yanhuai Highway in Huaiyin and Yancheng. The blockage events in the K710–K971 section of the G2 Beijing–Shanghai Highway and the K126–K261 section of the S28 Qiyang Highway reached a moderate level of six events in the central region of Suzhou.

There were fewer than two blockage events in the entirety of southern Jiangsu. The spatial distribution of highway blockages in Jiangsu Province in February showed a decreasing trend from north to south and from east to west, while the blockage events in March were mainly concentrated in the K819–K1736 section of the G25 Changshen Highway in the city of Huaiyin and in the K38–K136 section of the S18 Yanhuai Highway in the city of Yancheng in April. There was a sudden increase in the number of blockage events in May, mainly in the K890–K1093 section of the G15 Shenhai Highway along the eastern coast. Some blockage events occurred in the K854–K1087 section of the G15 Shenhai Highway in June but were substantially fewer than that in May. The number of highway-blocking events increased further in December. The highway-blocking events were still mainly concentrated in the coastal area and in the K854–K1087 section of the G15 Shenhai Highway, with 5–8 blockage events recorded in the K854–K1094 section. The K0–K206 section of the G30 Lianhuo Highway also had relatively high risk, with five to six recorded blockage events, while the number of highway blockages remained below two in southern Jiangsu.
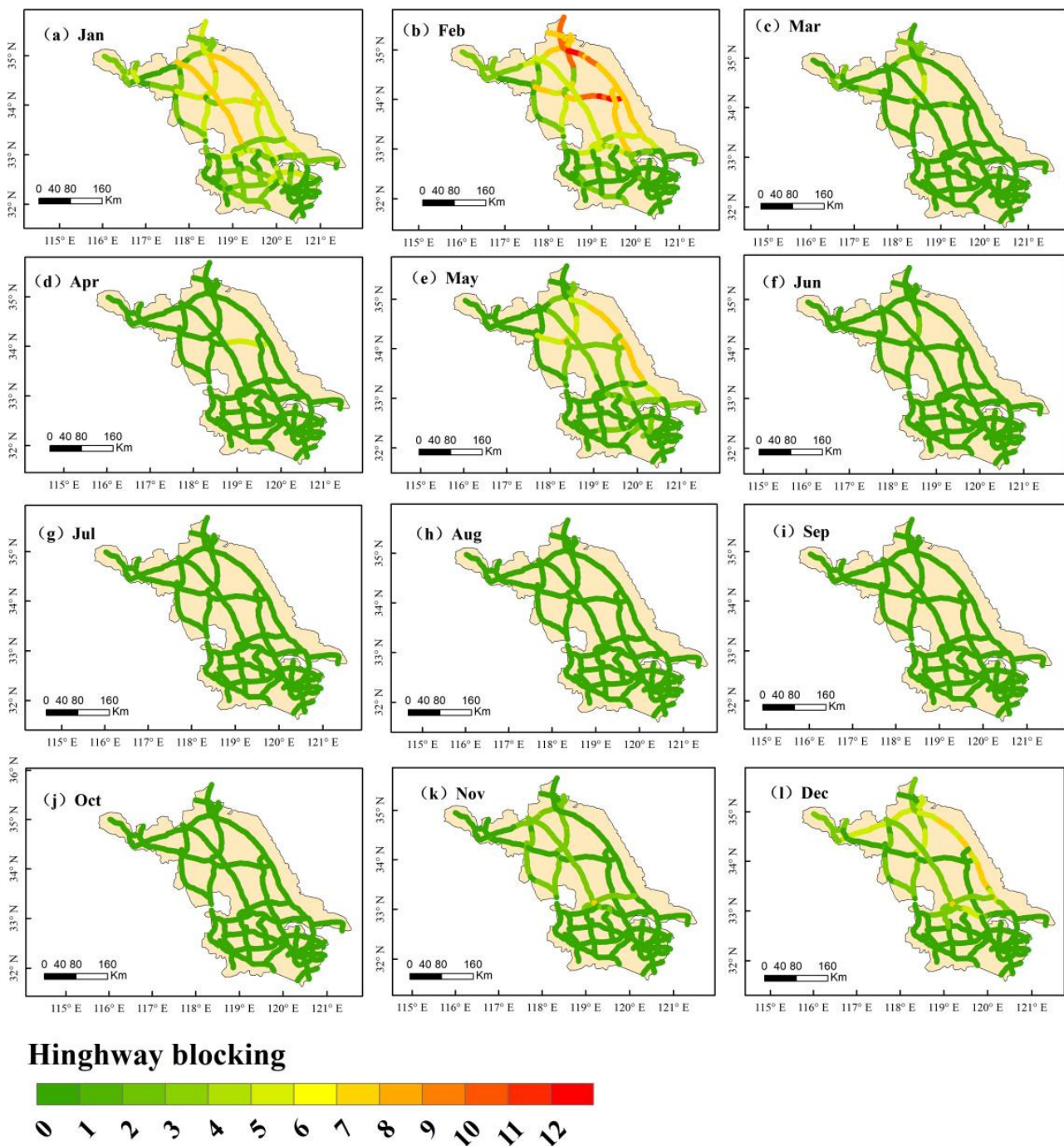
Figure 5. Annual variation of highway blockage distribution in Jiangsu Province in 2020.

3.1.2. Diurnal Variation of Highway-Blocking Events

As seen from the diurnal variation of the highway blockage frequency in Jiangsu Province in 2020 (Figure 6), highway-blocking events are mainly concentrated in the late night and early morning hours. The number of blockages reached the peak value between 00:00 and 01:00 Beijing time (BT) with the value of 158. From 00:00 to 04:00 BT, there was a decreasing trend in the frequency of highway blockages, and increased between 04:00 and 05:00 BT, reaching the second highest value of 135. The trend then decreased until 09:00 BT, with almost no blockage events from 10:00–21:00 BT. The number of blockage events started to increase after 21:00 BT and reached 130 at 23:00 BT. During the late night and

early morning hours, there was a greater number of events with blockage mileage over 200 km, as longer and more severe blockage events were common during this period.
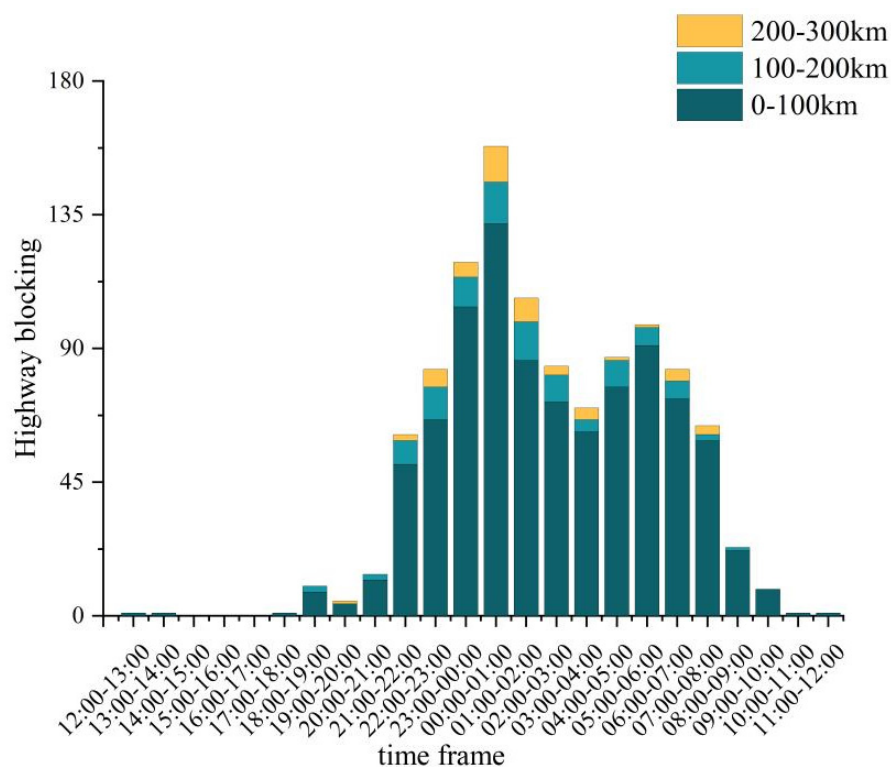

Figure 6. Diurnal variation of the annual average frequency of highway-blocking events in Jiangsu Province in 2020.

The spatial distributions of highway-blocking events during different time periods in Jiangsu Province in 2020 are shown in Figure 7. It shows that the highway-blocking events in Jiangsu Province are mainly concentrated between 00:00 and 08:00 BT. In general, the number of events in the north is higher than that in the south, and more events occur along the coast than inland. The overall trend shows the characteristic of decreasing from the eastern coast to the west, with the most highway-blocking events on the eastern coast and in the K888–K1004 section of the G15 Shenhai Highway. The section K744–K955 in the G2 Beijing–Shanghai Highway also has more highway-blocking events than average. During the period of 09:00–17:00 BT, the number of highway blockages in the entire province was relatively low; only the K765–K1098 section of the G15 Shenhai Highway and the K40–K140 section of the S18 Yanhuai Highway in the eastern coastal area had more than eight blockage events. There was an obvious increase in the number of highway blockages in the K0–K90 section of the G30 Lianhuo Highway in Lianyungang and the K1840–K1933 section of the G25 Changshen Highway in Huaiyin from 18:00–23:00 BT compared to the those during the period of 09:00–17:00 BT, showing an overall increasing trend from the inland to the eastern coastal area from 18:00–23:00 BT.
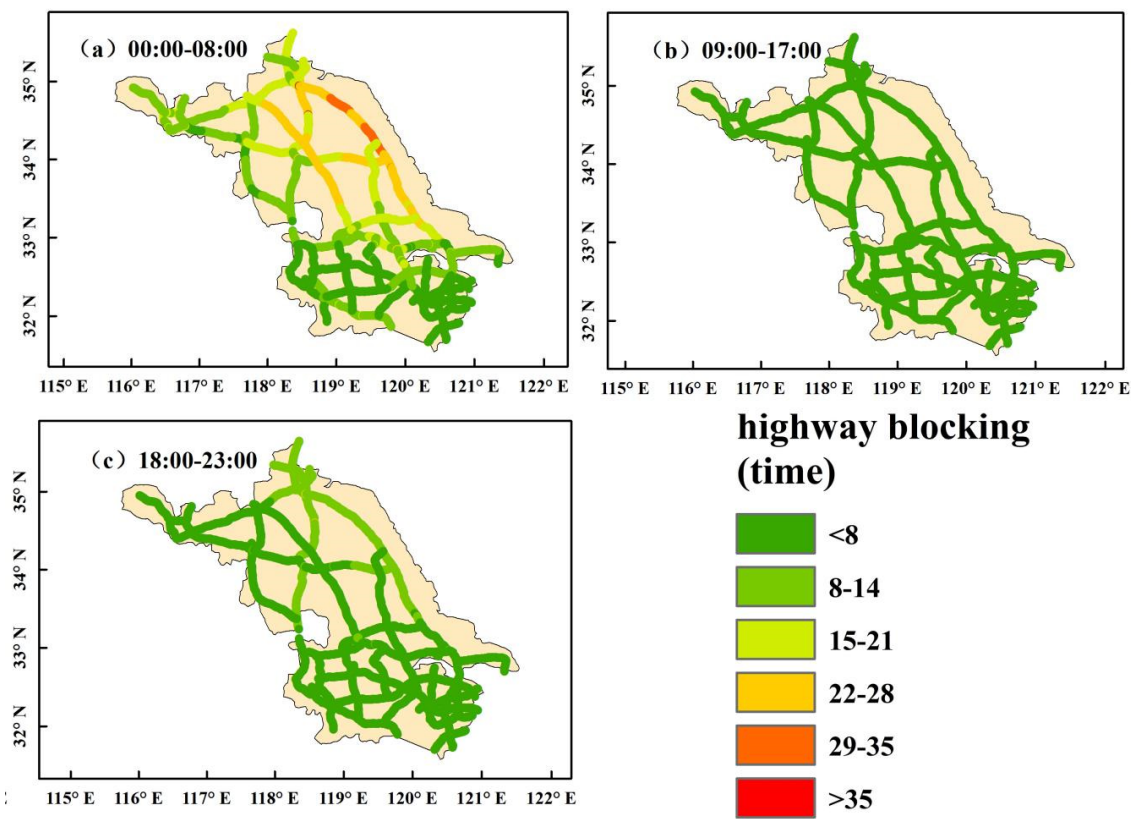
Figure 7. Spatial distributions of highway-blocking events during different time periods in Jiangsu Province, 2020.

3.2. Vulnerability of Highways to Low-Visibility Weather in Jiangsu Province

This study determines the vulnerability of each road unit in the Jiangsu provincial highway network to low-visibility weather by selecting data from the records of highway disruption events. The blockage frequency, the cumulative duration of blockage, the duration of blockage response, the duration of blockage rescue, and the duration of highway blockage with false alarm were used as the vulnerability indicators. The specific indicators are shown in Table 2.

Table 2. Indicators of highway network vulnerability assessment.

Target Level	Guideline Level	Number	Program Level	Number
Vulnerability	Sensitivity	A	Blockage frequency	A1
			Cumulative duration of blockage	A2
			Blockage severity	A3
	Emergency response capability	B	Duration of blockage response	B1
			Duration of blockage rescue	B2
			Duration of highway blockage with false alarm	B3

According to the indicator system in Table 2, the relative weights of the indicators corresponding to each fuzzy consistent judgment matrix were calculated using the characteristic root method to obtain the subjective weight. By unitizing the highway network data, the weight was calculated using the CRITIC method. The optimal weight allocation coefficients were determined to be those with the minimum standard deviation calculated using Equations (11) and (12). The results are shown in Figure 8, and the final weight *W* assignment was obtained using Equation (13). The final weights are shown in Table 3.

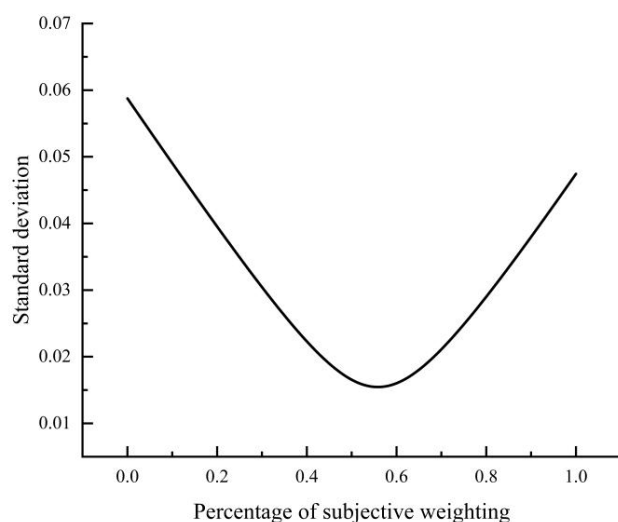$$W = 0.5583W_1 + 0.4417W_2 \tag{13}$$

Figure 8. Variation of standard deviation with weight coefficient of W_1.

Table 3. Weights of indicators for the vulnerability assessment.

Target Level	Guideline Level	Program Level	W_1	W_2	W
	Sensitivity	frequency of blockage	6.75%	28.34%	16.29%
		cumulative duration of blockage	17.57%	10.06%	14.25%
		Blockage severity	19.14%	11.65%	15.83%
Vulnerability	Emergency response capabilities	the duration of blockage response	21.99%	15.66%	19.19%
		Blocked rescue duration	17.87%	16.59%	17.30%
		the duration of highway blockages with false alarms	19.14%	17.71%	18.51%

.

First, each vulnerability index in Table 3 was calculated in a standardized way. Then, each vulnerability index of each road network unit was calculated. The final evaluation value was obtained according to W, and the evaluation results was matched to the highway network through GIS technology, as shown in Figure 9. It is obvious that the sensitivity of highway network in Jiangsu Province to low-visibility weather presents a decreasing trend from north to south. The vulnerability of highway network is higher in coastal areas and lower in southern Jiangsu. It is worth noting that the frequency of highway blockage in Nantong City is low, but the vulnerability is high, indicating poor capacity of disaster relief in this section. The S49 Suyang highway section in central Jiangsu is highly sensitive. Combined with the analysis of blockage events, the rescue response time of this section is relatively high. The high vulnerability of G30 Lianhuo Highway in Lianyungang City is mainly due to the high severity of a single highway-blocking event. For the highways in coastal areas, although the frequency of highway-blocking events is higher, the cumulative severity of highway blockage is lower, and the misreporting of highway blockage time is less. It indicates that the abilities of disaster resistance and emergency response are good in this area, which leads to a medium level of vulnerability. The density of the road network in the whole of southern Jiangsu is relatively high, but it is kept at a low vulnerability due to the low frequency of highway blockage in low-visibility weather.
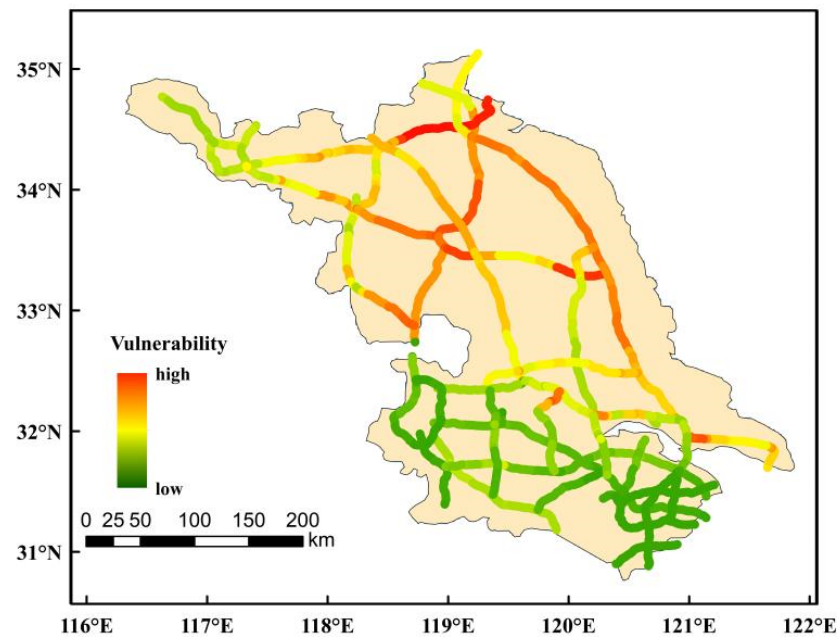
Figure 9. Distribution map of highway vulnerability in Jiangsu Province.

4. Discussion

4.1. Cause Analysis of the Blockage Distribution Due to Low-Visibility Weather

The reasons for the spatiotemporal distribution of highway-blocking events in Jiangsu Province were analyzed in relation to existing studies. Consistent with previous research, it has been observed that the hours between 00:00 and 04:00 BT are conducive to the occurrence of fog in Jiangsu Province; there is favorable environment of high air humidity, low wind speed, and cooling at nighttime.

Fog tends to last until 08:00 BT in the morning and begins to dissipate after sunrise, when the solar radiation increases, the temperature near the ground rises, and the relative humidity of the air decreases. This is one of the reasons that contribute to the sharp decline in the blockage events related to low-visibility weather starting at 08:00 BT [40].

Generally, after 10:00 BT, the wind speed at ground level gradually increases until approximately 14:00 BT, when it reaches the maximum value for the day. Aerosol particles in the air are also more likely to disperse during this period. Therefore, the probability of low-visibility weather is lower, and the number of highway-blocking events begins to decrease accordingly [41]. When the lighting condition is better in the afternoon, the visibility is less likely to be affected and to drop low enough to cause highway blockage, which makes the occurrence of blockage events less frequent.

In the coastal area of northern Jiangsu, the topography is more complex, and surface water is more widely available. Coastal geography also provides abundant water vapor and appropriate conditions for the formation of fog [42,43]. As a result, the frequency of highway blockage due to low visibility in the coastal area of northern Jiangsu is higher year-round.

In summary, the seasonal distribution of highway-blocking events in Jiangsu obviously shows fewer events in summer and more events in winter which is consistent with the seasonal distribution of low-visibility weather. The diurnal variation of highway-blocking events shows that more events occur in the nighttime and that fewer occur in the daytime.

4.2. Vulnerability Assessment and Analysis of Highway Network in Low-Visibility Weather

In this study, the highway network was segmented into units by GIS technology, and the highway-blocking events from the highway blockage data record table were matched with the road network information by matching function. Highway-blocking events can be

quickly positioned on specific units, and the spatial distribution map of blockage events can be effectively obtained.

The blockage events that have happened on each road network unit were sorted out and analyzed, and the comprehensive weight assignment method combining the FTHP and CRITIC methods was adopted to calculate the blockage event information of each road unit, and the final vulnerability assessment result of the entire highway network in Jiangsu Province to low-visibility weather was obtained. The result can be used to effectively avoid traffic blockage in practice and provide reference for road safety operation management.

The distribution of road network vulnerability to low-visibility weather in Jiangsu Province is higher in the north and lower in the south. The coastal and central regions are more vulnerable than the southern inland regions. Among them, the highways in coastal areas have higher frequencies of blockage events, but their overall vulnerability is at a medium level due to the high capability of disaster resistance and emergency response. In the whole network, the vulnerability is higher at the intersections of highways.

In the whole highway network, the vulnerability of east–west highways—such as highways G30 and S18—which have poor performance in disaster preparedness is higher. The northern part of G30 is the worst in terms of disaster resilience. In addition, highway G25 in the north is highly sensitive, which leads to higher vulnerability. It is worth noting that although the annual blockage frequency of G40 in Nantong City is low, the overall vulnerability also reaches a medium level due to the long false alarm blockage time in this section.

Studies on motorway disruptions in low-visibility weather have focused more on the traffic flow and travel mode chosen by drivers [44,45]. Chaudhuri et al. [46] used the 10-year motorway accident data in Barcelona to build a risk model for the urban motorway network through Bayesian networks. However, accidents are contingent, and a single high damage accident can affect the risk assessment results of the whole network. In contrast, the traffic-blocking events used in this study have covered a wider range, taking traffic congestion in low-visibility weather into account, and can reduce the impact of a single event to a certain extent.

Miomir et al. [47] used the fuzzy MARCOS method to analyze accident risk at 38 points along a 7.3 km stretch of road, which is better for shorter roads but is not applicable to the emergency preparedness planning and design for the whole road network. Some scholars used accident data in their studies of road traffic risk and vulnerability, which are inextricably linked to drivers, and some have also studied the characteristics of drivers in traffic accidents.

It is therefore difficult to define whether the specific factors that contribute to each accident are external environmental factors or the internal factors of drivers in the study of highway accidents. In contrast, the traffic-blocking events are based on field record data, which allows for a clearer identification of the weather factors that led to the blockage.

It is worth noting that the geographical environment of the specific highway was not taken into account in this study for the vulnerability modelling process. However, in the analysis of road traffic risk, the presence of bridges and tunnels, as well as the road gradient and road surface material, are also important reference indicators which will be considered in the analysis of key blocked sections in the future study.

4.3. Prevention and Control Measures in the Sections with High Blockage Frequency

In this study, we have selected the three most severely blocked highways, G15, G2, and G25, which need the focus of attention of meteorological and traffic authorities. The blocked sections in these highways were classified into three levels according to the number of highway-blocking events: lighter, medium, and serious (Table 4). The meteorological department should prepare forecasts for low-visibility weather, and the transport department should prepare in advance for low-visibility weather. Additional warning signs should be erected on the blocked roads to remind drivers to pay attention to current road conditions and slow down. On the other hand, light-emitting diode (LED) fog lights and monitoring

equipment should be installed in the sections prone to severe low-visibility blockages, and reserve ramps should be built in excessively long sections prone to blockage to clear the traffic flow in the low-visibility weather. Staff and duty points should be arranged to be on duty in advance in the blockage-prone periods and sections. Additional weather stations are also needed to enhance monitoring capability. In the lighter-level sections, the density of monitoring stations should be improved to 10 km per station, while the density for the sections of medium and serious levels needs to be increased to 5 km per station. Appropriate emergency plans and rescue measures for different levels of traffic-blocking events also need to be improved. It is important to warn drivers before the occurrence of blockage, and contact drivers in time to strengthen the diversion of traffic flow after the end of blockage.

Table 4. Actions suggested by the traffic department.

Route Number	Highway Blockage	Highway Blockage Section	Fog Lights Suggestions	Road Proposal
G15	lighter	K1164–K1184	Unidirectional mounting	Place warning signs
		K1217–K1251		
		K823–K835		
	medium	K1182–K1216		Diversion road
		K760–K822		Diversion road
		K836–K844	Bidirectional installation	Place warning signs
	serious	K846–K1163		Diversion road
		K2122–K2190		Place warning signs
G2	lighter	K1089–K1190	Unidirectional mounting	Diversion road
		K972–K991		Place warning signs
		K1039–K1088		
	medium	K710–734	Bidirectional installation	Place warning signs
		K979–K1061		Diversion road
	serious	K735–K970		Place warning signs
G25	lighter	K1644–K1693	Unidirectional mounting	Place warning signs
	medium	K1827–K1932	Bidirectional installation	Diversion road
		K1763–1825		Place warning signs
	serious	K1695–K1760		

5. Conclusions

This study used the traffic blockage data of highways in Jiangsu Province in 2020 to identify and locate highway-blocking events for individual highway marker. By using the Python programming language, GIS technology and mathematical statistics, the spatiotemporal distribution characteristics of highway-blocking events in Jiangsu Province were analyzed, and the vulnerability of Jiangsu highway network to low-visibility weather was assessed through the FAHP and CRITIC weight assignment methods. The main conclusions are as follows.

Jiangsu Province has a distinct seasonal variation of highway blockage with a bimodal pattern of annual variation. Blockage events are more likely to occur in winter, followed by spring and autumn, and they are less likely to occur in summer. Most highway-blocking events occur during late night to early morning, followed by early evening, with minimal occurrence in the afternoon. The peak time of blockage occurrence is during 00:00–01:00 BT, with no blockage occurring during 09:00–21:00 BT.

More highway-blocking events occur in the north of Jiangsu Province than in the south, and more blockage events occur in the eastern coast than in the western hinterland,

which indicates an overall decreasing trend from the coastal area to inland. Lianyungang and Yancheng are the cities with the highest incidence of highway blockage, whereas the most blockage events occur on the G15 Shenhai highway in the coastal area.

The main distribution characteristic of vulnerability for the highways in Jiangsu Province is higher in the north and lower in the south. The vulnerability of highways in coastal areas is higher than in inland areas. Among them, the K2122–K2190 section of the G25 Shenhai Highway, the K735–K970 section of the G2 Beijing–Shanghai highway, the K1595–K1760 section of the G25 Changshen Highway, and the K6–K99 section of the G30 Lianhuo Highway are highly sensitive to low-visibility weather. The primary factors of high vulnerability are different in different regions. Northern Jiangsu is dominated by high sensitivity and low capabilities of disaster resistance and emergency response, while central Jiangsu is dominated by the capabilities of disaster resistance and emergency response. The vulnerability of highways in southern Jiangsu is at low level due to the few blockage events.

It is important to note that the time series of the highway blockage data used in the study is relatively short, with only 1-year data available (2020), which imposes certain limitations on the reliability of our results. It is expected that a longer time series will be available in the future to verify the spatiotemporal distributions obtained from the analysis presented here. Furthermore, the quantitative analyses of the spatial and temporal variabilities of highway-blocking events cannot be conducted due to the complexity of road environment factors, while only qualitative analyses can be conducted through literature research, practical investigation, and professional knowledge. Currently, it is not possible to quantitatively analyze the characteristics and causes of highway-blocking events by combining various meteorological elements and geographic environmental factors, which must be continuously improved in the future.

Author Contributions: Conceptualization, T.J. and D.L.; methodology, D.L. and Y.B.; investigation, H.W. and M.Y.; resources, M.Y.; data curation, F.Z.; writing—original draft preparation, T.J.; writing—review and editing, D.L. and Y.B. All authors have read and agreed to the published version of the manuscript.

Institutional Review Board Statement: Not applicable.

Informed Consent Statement: Not applicable.

Data Availability Statement: Data available on request due to restrictions, e.g., privacy or ethical; the data presented in this study are available on request from the corresponding author. The data are not publicly available due to confidentiality.

Conflicts of Interest: The authors declare no conflict of interest.

References

1. Huang, C.F. The basic principle of integrated risk assessment. In Proceedings of the First International Conference on Risk Analysis and Crisis Response, Shanghai, China, 25–26 September 2007; pp. 22–27.
2. Ministry of Transport of the People's Republic of China. *Traffic Blocking Information Reporting System of Ministry of Transport (Trial Operation, Ministry of Transport)*; Ministry of Transport of the People's Republic of China: Beijing, China, 2006.
3. The Ministry of Transport of the People's Republic of China. *Traffic Blocking Information Reporting System of the Ministry of Transport*; The Ministry of Transport of the People's Republic of China: Beijing, China, 2011.
4. Song, J.; Li, Y.; Zhang, H.; Tian, H.; Cheng, Z.; Yi, X. Analysis of the Influence of Severe Weather on Highway Traffic Blocking. *Highway* **2021**, *66*, 248–256.
5. Yan, K.; Dong, L. Data Statistics and Analysis of Blocked Road Information in China. *J. Highw. Transp. Res. Dev.* **2009**, *16*, 121–124.
6. Zhang, Y.; Ou, B.; Sun, X. Cause analysis and solution of highway traffic accident in foggy weather. *China Sci. Technol. Inf.* **2008**, *20*, 294.
7. Yan, M. The Charaeteristies and Numerical Simulations of Dense Fog Along Nanjing To Shanghai highway. Master's Thesis, Nanjing University of Information Science & Tcchnology, Nanjing, China, 2011.
8. Huang, B. Study on the Traffic Risk Analysis and Forewarning Management of Freeway Under Disaster Weather. Master's Thesis, Shanghai Jiao Tong University, Shanghai, China, 2012.

9. Gao, Y.; Gong, J. Characteristics and mechanism of road traffic accidents. *J. Saf. Environ.* **2022**, *6*, 12–15. [CrossRef]
10. Zhang, J.; Tan, G.; Wu, H.; Zhang, Y.; Zhang, D. Characteristics on Highway Traffic Accidents Caused by the Disastrous Weather in Hebei and the Early-warning Indexes System of Highway Traffic Under Foggy Weather Condition. *J. Arid Meteorol.* **2016**, *34*, 370–375.
11. Wang, Y.; Liang, L.; Evans, L. Fatal crashes involving large numbers of vehicles and weather. *J. Safety Res.* **2017**, *63*, 1–7. [CrossRef]
12. Hamilton, B.; Tefft, B.; Arnold, L.; Grabowski, J. Hidden highways: Fog and traffic crashes on America's roads. 2014. Available online: http://aaafoundation.org/wp-content/uploads/2017/12/FogAndCrashesReport.pdf (accessed on 13 March 2023).
13. Abdel-Aty, M.; Ekram, A.A.; Huang, H.; Choi, K. A study on crashes related to visibility obstruction due to fog and smoke. *Accid. Anal. Prev.* **2011**, *43*, 1730–1737. [CrossRef]
14. Al-Ghamdi, A.S. Experimental evaluation of fog warning system. *Accid. Anal. Prev.* **2007**, *39*, 1065–1072. [CrossRef]
15. Perry, A.H. *Environmental Hazards in the British Isles*; George Allen & Unwin: London, UK, 1982; p. 73.
16. Wu, Y.; Abdel-Aty, M.; Lee, J. Crash risk analysis during fog conditions using real-time traffic data. *Accid. Anal. Prev.* **2017**, *114*, 4–11. [CrossRef]
17. Feng, L.; Deng, Y.; Li, A.; Li, Y.; Song, J. The characteristics of traffic accidents in highway in fog days and their relationship with visibility. *Sci. Technol. Rev.* **2020**, *38*, 160–168.
18. Edwards, J.B. The temporal distribution of road accidents in adverse weather. *Meteorol. Appl.* **1999**, *6*, 59–68. [CrossRef]
19. Berdica, K. An introduction to road vulnerability: What has been done, is done and should be done. *Transp. Policy* **2002**, *9*, 117–127. [CrossRef]
20. Husdal, J. The vulnerability of road networks in a cost-benefit perspective. In Proceedings of the Transportation Research Board Annual Meeting (TRB 2005), Washington, DC, USA, 9–13 January 2005.
21. Sohn, J. Evaluating the significance of highway network links under the flood damage: An accessibility approach. *Transp. Res. Part A Policy Pract.* **2006**, *40*, 491–506. [CrossRef]
22. Scott, D.M.; Novak, D.C.; Aultman-Hall, L.; Guo, F. Network robustness index: A new method for identifying critical links and evaluating the performance of transportation networks. *J. Transp. Geogr.* **2006**, *14*, 215–227. [CrossRef]
23. Huang, H.; Chin, H.C.; Haque, M.M. Severity of driver injury and vehicle damage in traffic crashes at intersections: A Bayesian hierarchical analysis. *Accid. Anal. Prev.* **2008**, *40*, 45–54. [CrossRef] [PubMed]
24. Cherry, C.R.; Weinert, J.X.; Xinmiao, Y. Comparative environmental impacts of electric bikes in China. *Transp. Part D Transp. Environ.* **2009**, *14*, 281–290. [CrossRef]
25. Williams, A.F.; Shabanova, V.I. Responsibility of drivers, by age and gender, for motor-vehicle crash deaths. *J. Saf. Res.* **2003**, *34*, 527–531. [CrossRef]
26. Yu, R.; Quddus, M.; Wang, X.; Yang, K. Impact of data aggregation approaches on the relationships between operating speed and traffic safety. *Accid. Anal. Prev.* **2018**, *120*, 304–310. [CrossRef]
27. De Ona, J.; López, G.; Mujalli, R.; Calvo, F.J. Analysis of traffic accidents on rural highways using Latent Class Clustering and Bayesian Networks. *Accid. Anal. Prev.* **2013**, *51*, 1–10. [CrossRef]
28. Kashani, A.T.; Mohaymany, A.S. Analysis of the traffic injury severity on two-lane, two-way rural roads based on classification tree models. *Saf. Sci.* **2011**, *49*, 1314–1320. [CrossRef]
29. Harb, R.; Yan, X.; Radwan, E.; Su, X. Exploring precrash maneuvers using classification trees and random forests. *Accid. Anal. Prev.* **2009**, *41*, 98–107. [CrossRef] [PubMed]
30. Cannon, T.; Twigg, J.; Rowell, J. Social Vulnerability, Sustainable Livelihoods and Disasters. *Benfield Hazard Res. Cent.* **2003**, *93*, 22. Available online: https://www.researchgate.net/profile/J-Twigg/publication/254398816_Social_Vulnerability_Sustainable_Livelihoods_and_Disasters/links/56656a1308ae4931cd621574/Social-Vulnerability-Sustainable-Livelihoods-and-Disasters.pdf (accessed on 13 March 2023).
31. Li, X.; Xiao, G.R.; Cai, S.H. Evaluation of water environmental sensitivity based on fuzzy analytic hierarchy process combined with web text. *J. Geo-Inf. Sci.* **2019**, *21*, 1832–1844. Available online: http://www.dqxxkx.cn/CN/10.12082/dqxxkx.2019.190165 (accessed on 13 March 2023).
32. Qi, Q.S.; Yang, Z.L. GRA and CRITIC Method for Intuitionistic Fuzzy Multiattribute Group Decision Making and Application to Development Potentiality Evaluation of Cultural and Creative Garden. *Math. Probl. Eng.* **2021**, *2021*, 9957505. [CrossRef]
33. Kumar, A.; Sharma, M.P.; Rai, S.P. A novel approach for river health assessment of Chambal using fuzzy modeling, India. *Desalination Water Treat.* **2017**, *58*, 72–79. [CrossRef]
34. Gong, Q.; Chen, B.Z.; Zhi, P.P.; Li, Y.H. Comprehensive Evaluation for Design for Design Scheme of Metro Auxiliary Power supply System Based on FAHP. *IOP Conf. Ser. Mater. Sci. Eng.* **2021**, *2*, 1043. [CrossRef]
35. Wu, Z.R. The Application of FAHP in Decisions of Pavement Maintenance. *IOP Conf. Ser. Earth Environ. Sci.* **2017**, *1*, 61. [CrossRef]
36. Jakiel, P.; Fabianowski, D. FAHP model used for assessment of highway RC bridge structural and technological arrangements. *Expert Syst. Appl.* **2015**, *42*, 4054–4061. [CrossRef]
37. Zhong, S.H.; Chen, Y.; Miao, Y.J. Using improved CRITIC method to evaluate thermal coal suppliers. *Sci. Rep.* **2023**, *13*, 195. [CrossRef]
38. Sun, B.; Yu, H.X.; Liu, B.J. Initial Water Rights Allocation in Hanjiang District of Meizhou City Based on Improved CRITIC Method. *Water Resour. Power* **2022**, *40*, 61–65. [CrossRef]

39. Niu, S.; Liu, J.; Li, Y.; Sha, H.; Zhang, J. Data analysis method of blocked road information based on GIS. *J. Chang. Univ.* **2015**, *35*, 211–215. [CrossRef]
40. Zong, C.; Qian, W.; Bao, Y.; Yuan, C.; Zhou, L.; Cui, C.; Wang, H. Temporal-Spatial Variations of Summerdense fog and Its Meteorological Influence Factors in Jiangsu Province. *Meteorol. Mon.* **2019**, *45*, 968–977.
41. Cao, J.; Guo, P. Feature analysis of fog concentration and climatic tendency of Jiangsu province. *J. Meteorol. Sci.* **2016**, *36*, 632–638.
42. Wang, B.; Pu, M.; Tian, L.; Zhang, Z.; Wu, J. Climate Characteristics and Impact Factors of Low-Visibilitydense fog on Jiangsu Coast highway. *Meteorol. Mon.* **2016**, *42*, 192–202.
43. Yu, G.; Wang, B.; Chen, P.; Huang, L.; Xie, X. Analysis of Characteristics of a Long-Lasting Fog-Haze Event in Jiangsu 2013. *Meteorol. Mon.* **2015**, *41*, 622–629.
44. Liu, Y.; Huang, X.; Duan, J.; Zhang, H. The assessment of traffic accident risk based on grey relational analysis and fuzzy comprehensive evaluation method. *Nat. Hazards* **2017**, *88*, 1409–1422. [CrossRef]
45. Zhu, C. The Method of Road Traffic Risk Assessment. *IOP Conf. Ser. Mater. Sci. Eng.* **2020**, *768*, 032001. [CrossRef]
46. Chaudhuri, S.; Saez, M.; Varga, D.; Juan, P. Spatiotemporal modeling of traffic risk mapping: A study of urban road networks in Barcelona, Spain. *Spat. Stat.* **2023**, *53*, 100722. [CrossRef]
47. Stanković, M.; Stević, Ž.; Das, D.K.; Subotić, M.; Pamučar, D. A New Fuzzy MARCOS Method for Road Traffic Risk Analysis. *Mathematics* **2020**, *8*, 457. [CrossRef]